Journal of Chromatography A, 1432 (2016) 92–100

Contents lists available at ScienceDirect

Journal of Chromatography A

journal homepage: www.elsevier.com/locate/chroma

Multimethod approach for the detection and characterisation of food-grade synthetic amorphous silica nanoparticles

Francisco Barahona, Isaac Ojea-Jimenez, Otmar Geiss, Douglas Gilliland, Josefa Barrero-Moreno*

European Commission, Joint Research Centre, Institute for Health and Consumer Protection, Via E. Fermi 2749, 21027 Ispra, VA, Italy

ARTICLE INFO

Article history:
Received 18 August 2015
Received in revised form
16 December 2015
Accepted 20 December 2015
Available online 23 December 2015

Keywords:
Silica nanoparticle
AF4
ICP-MS
DLS
TEM
Food-grade

ABSTRACT

Synthetic amorphous silica (SAS) has been used as food additive under the code E551 for decades and the agrifood sector is considered a main exposure vector for humans and environment. However, there is still a lack of detailed methodologies for the determination of SAS' particle size and concentration. This work presents the detection and characterization of NPs in eleven different food-grade SAS samples, following a reasoned and detailed sequential methodology. Dynamic Light Scattering (DLS), Multiangle Light Scattering (MALS), Asymmetric Flow-Field Flow Fractionation (AF4), Inductively Coupled Plasma Mass Spectrometry (ICPMS) and Transmission Electron Microscopy (TEM) were used. The suitability and limitations, information derived from each type of analytical technique and implications related to current EC Regulation 1169/2011 on the provision of food information to consumers are deeply discussed. In general the z-average, AF4 hydrodynamic diameters and root mean square (rms) radii measured were in good agreement. AF4-ICPMS coupling and pre channel calibration with silica NPs standards allowed the reliable detection of NPs below 100 nm for ten of eleven samples (AF4 diameters between 20.6 and 39.8 nm) and to quantify the mass concentration in seven different samples (at mg L^{-1} concentration level). TEM characterisation included the determination of the minimum detectable size and subsequent measurement of the equivalent circle diameter (ECD) of primary particles and small aggregates, which were between 10.3 and 20.3 nm. Because of the dynamic size application range is limited by the minimum detectable size, all the techniques in this work can be used only as positive tests.

1. Introduction

Silica, and specifically synthetic amorphous silica (SAS), has been used in the food industry sector as food additive under the code E551 for decades. The most frequent functions of SAS as E551 usually are anticaking agent, antifoaming agent or flow aid in powdered food, but it is also used for other applications during the food processing such as clarifying/fining agent in the juice, oil and brewery sector or as flavour/aroma carrier [1]. This widespread use increases the possibility of the occurrence of anthropogenic silica nanoparticles (NPs) in various environmental compartments [2,3] and the agrifood sector has been identified as one of the main exposure vectors for both humans and environment [4].

SAS is produced synthetically by either a vapour-phase process yielding pyrogenic (or fumed) SAS, or by a wet process yielding precipitated silica or silica gel. Related to this, although composition and purity criteria for food additives are described in the European Commission Directive 2008/84/EC, applying also to E551, there is no mention of size or dimensional requirements [5]. In this regard, recent Regulation 1169/2011 on the provision of food information to consumers [6], which came into force on December 14th 2014, includes a specific definition of engineered nanomaterial (ENM). Such a definition, in contrast to the EC Recommendation on the definition of nanomaterial 2011/696, does not include any established threshold in the number of particles (neither in mass nor number) with at least one dimension below 100 nm [7]. Hence, currently according to a strict interpretation of the Regulation 1169/2011 on the provision of food information to consumers an ingredient should be considered ENM if NPs are detected, independently of its number fraction. With regard to the case of SAS, producers of food-grade SAS often provide information about the particle size and describe the material as agglomerates formed from aggregates of covalently bound primary particles. Although some authors have reported on the detection and characterisation of silica (SiO_2)-NPs in food [8–11], in general there is still a lack of detailed methodologies for the detection, and characterisation

* Corresponding author.
E-mail address: Josefa.BARRERO@ec.europa.eu (J. Barrero-Moreno).

http://dx.doi.org/10.1016/j.chroma.2015.12.058

of SAS' particle size. In this regard, dynamic light scattering (DLS) is a valuable sizing technique present in many laboratories and often used to characterise and evaluate suspensions of nanoparticles due to the simplicity of handling and operation, as well as potentially good repeatability for monomodal samples [12]. For instance, it has been used as measuring technique in validation and interlaboratory studies [13,14] and in the development of size reference materials [15]. However, DLS is less suitable for multimodal samples or for broad size distributions. Furthermore, DLS is not a selective technique and, on the contrary, provides an overall size for all the particulate in suspension. Therefore, depending on particular needs, DLS is considered as a complementary technique to be used together with others. Field-Flow Fractionation (FFF) techniques, such as Sedimentation Field-Flow Fractionation (SdFFF) and Asymmetric Flow Field-Flow Fractionation (AF4), are powerful separation techniques well suited for the characterization of NPs in complex matrixes [16–18], including food and environmental samples [19–23]. Changing the separation settings, the dynamic size range of application can be modified. If appropriate calibration of the channel is performed, it is also possible to obtain accurate information on the size of the eluting particles [24]. Moreover, depending on the detector coupled to the AF4 instrument, it is possible to collect additional information of particle size and concentration. Related to this, Multi Angle Light Scattering (MALS) is often coupled to AF4 and used as detector, as it can provide independent information about the NPs' size [25]. AF4 separation can be also coupled to inductively coupled plasma mass spectrometry (ICPMS), thus combining the advantage of AF4's ability to separate NPs according to their hydrodynamic diameter with the excellent sensitivity and selectivity of ICPMS detection [26]. Each measuring technique exhibits its own advantages and limitations, and derived information should be interpreted carefully [27]. A combined use of all of them following a multimethod approach has been sometimes proposed since the information from each individual method is usually complementary [28–30].

In the present work a systematic sequential evaluation scheme that involves the use of different techniques is proposed for the assessment on the presence of NPs in food-grade SAS. Different samples received from some of the main producers of food-grade SAS have been characterised in their dispersed form in water, in the framework of the Regulation on the provision of food information to consumers. The use of DLS, AF4-MALS and AF4-ICPMS has been proposed as they are commonly applied to the characterisation of nanomaterials. Last, but not least, Transmission Electron Microscopy (TEM) analysis was also applied for particle size characterisation and to compare the results obtained by previous techniques. The suitability and type of information derived from every type of analysis has been discussed.

2. Materials and methods

2.1. Chemicals

The following chemicals were obtained from Sigma–Aldrich (Sigma–Aldrich Corp., St. Louis, USA): ammonium carbonate (product code 379999), nitric acid (product code 84385), silicon standards for ICPMS (code 08729). Water used in all the experiments was Milli-Q® ultrapure grade water.

2.2. Nanoparticles standards

SiO_2-NPs (NanoSilica™ Size Standards) with 20, 40, 60, 80, 100 and 150 nm nominal diameters, respectively, were purchased from MSP Corporation (Shoreview, MN, USA). SiO_2-NPs with 0.49 μm (8000 Series Silica Particle Size Standards) were obtained from Thermo (ThermoFischer Scientific, Waltham, MA, USA). SiO_2-NPs standards were used for AF4 calibration.

Stock suspensions were stored in dark and following the supplier's recommendations. Dilutions and working suspensions from the stock materials were freshly prepared each week.

2.3. Dispersion and filtration of food-grade synthetic amorphous silica samples

All SAS samples under study were voluntarily donated from suppliers after request. Eleven different types of SAS were received and subsequently subjected to characterisation. SASs in the form of powder were exactly weighted (approximate 300 mg) in a 50 mL polypropylene tube and 25 mL of ultrapure water added. The tube was vortex-stirred for 10 s and sonicated for 10 min using a 130 Watt Ultrasonic Processor equipped with a 6 mm probe from Sonics, (Sonics & Materials, Inc., Newtown, CT, USA), which operated at 50% amplitude (theoretical input to sonicator was 8000 J). A 2 mL aliquot of the original suspensions was filtered through 0.45 μm membrane filters (Millex®-HV, i.d. 25 mm, PVDF) using a vacuum manifold operating at 16 inc Hg.

2.4. Dynamic light scattering

A Zetasizer Nano-ZS, (Malvern, England) was used to perform dynamic light scattering (DLS) measurements. Measurements of the just-prepared stock suspensions were performed in triplicate immediately after preparation, using 1 mL disposable sizing cuvettes at 25 °C. DLS settings included automatic optimisation of the measurement position and automatic selection of attenuator. All samples were stored in their respective sizing cuvettes for 24 h and measurements were repeated under identical settings without stirring or shaking the suspensions. The analyses of the filtered samples were performed with identical settings after the immersion of the filtrates in an ultrasound bath for ten minutes.

2.5. Characterisation of synthetic amorphous silica samples by transmission electron microscopy

TEM (JEOL JEM 2100, Japan) at an accelerating voltage of 200 kV was used to visualize the nanoparticles. Ultrathin Formvar-coated 200-mesh copper grids (Tedpella Inc.) were previously functionalized by placing the carbon-coated side on a drop of about 20 μL of Alcian blue (2 % in water) placed on a parafilm and incubating for 10 min. The grid was then washed by transferring it to 5 drops of water placed on a parafilm and the excess fluid was removed by blotting its edge on a strip of paper tissue, leaving a trace of humidity. Finally the grid was placed on a 20 μL drop of the corresponding dispersion, incubated for 10 min and excess of fluid removed again with a paper tissue. Digital images were analyzed with the ImageJ software and a custom macro without background subtraction, smoothing nor separation of touching particles, using manual global threshold settings and varying the minimal size provided by ImageJ. No circularity filter was used to exclude agglomerates. The macro can be downloaded from http://code.google.com/p/psa-macro For each sample, the size of at least 200 particles was measured to obtain the average and the size distribution.

2.6. Elemental analysis of silica nanoparticles by ICPMS

The elemental analysis was performed using a PerkinElmer NexIon 300D quadrupole ICPMS, equipped with a SC Fast peristaltic pump, a Meinhard concentric nebulizer, a glass cyclonic spray chamber and a standard quartz torch (2.5 mm i.d). The system operated in standard mode monitoring isotopes m/z 28 and 29 for Si with

dwell time of 50 ms and integration time of 1 s. The quantification was performed by external calibration with silicon standards for ICP (TraceCert, Sigma–Aldrich). Reported values were the average result of 5 measurements.

2.7. On-line AF4-MALS-ICPMS coupling: separation and elemental analysis of silica nanoparticles

A previous work reported a detailed method for the separation and analysis of SiO_2-NPs in aqueous samples by AF4-MALS-ICPMS [4]. The AF4 instrument comprised an Eclipse Dualtec Separation System from Wyatt Technology Europe and an Agilent 1260 Infinity high performance liquid chromatograph (HPLC) equipped with a degasser (G1322A); an Isocratic pump (G1310B); an autosampler (G1329B); a multi wavelength detector (G1365C), from Agilent Technologies. A DAWN 8$^+$ Heleos II multi-angle light scattering (MALS) detector operating with a 658 nm laser (Wyatt Technology) was coupled to the fractionation system and the 90° angle was used to monitor the signal. A pre-cut 10 kDa regenerated cellulose membrane and a 350 μm height spacer were assembled inside the Eclipse SC channel 153 mm length, which was located inside a Thermos [PRO] thermostatic unit, all from Wyatt Technologies. The temperature was set at 25 °C. The eluent consisted of a 0.25 mM ammonium carbonate aqueous solution which was freshly prepared every day. Processing of AF4-MALS data was performed using ASTRA® 6.1 software (Wyatt Technology)

In order to acquire the on-line ICPMS signal, the AF4 detector flow-outlet tube was connected directly to the ICPMS nebuliser inlet. Isotope Si28 was monitored with dwell time of 50 ms and integration time of 1 s. The raw data were converted into. xlx file for subsequent integration of peak areas using the Peak Analyser tool present in OriginPro8® software (OriginLab Corporation, USA).

Two different set of conditions were used for AF4 separation using cross-flow rates of 0.15 mL min^{-1} and 1.0 mL min^{-1}, respectively. In the first method the separation was calibrated with 100 and 490 nm SiO_2-NPs. The second method was calibrated for size and concentration using previously characterised monodispersed SiO_2-NPs standards of 20, 60 and 100 nm, as detailed somewhere else [31]. Experimental limits of detection were 0.16, 0.16 and 0.20 mg L^{-1}, respectively. Hydrodynamic diameters (AF4 diameters) were calculated using the elution time at peak maximum. The detector flow was set at 0.5 mL min^{-1} in every case.

3. Results and discussion

As discussed previously, a multimethod approach for NP detection and sizing in food-grade SAS samples in the form of dispersion is proposed here. An overview of the sequential evaluation scheme (see Fig. S1) includes: (1) preparation of aqueous suspension and DLS measurement; (2) filtration and subsequent DLS measurement of filtrates; (3) AF4-MALS analysis of filtrates; (4) AF4-ICPMS analysis of filtrates; (5) TEM characterization of suspensions. The sequential order in which the techniques are used is primarily based on the requirement of increasing the amount of information, achieving better resolution and greater sensitivity, but also on the increasing complexity, duration of analysis and cost. The discussion of the results after each type of analysis is discussed below.

3.1. Suspension and preparation of samples

To perform DLS measurements and to prepare the samples for TEM as well as for flow analysis, powder materials like SAS must be dispersed in liquid medium. Hence, it was decided to establish a sample preparation protocol and characterise the materials accordingly dispersed. Although the preparation of the sample certainly impacts on the particle size distribution (PSD) of the materials [32,33], neither the impact of the dispersing protocol nor the filtration process on the samples' PSDs was studied in this work. The dispersion protocol was adapted from a previous comparison study in which the particle size of fumed SAS was studied [34]. To favour repeatability, the use of the ultrasonic probe as dispersing technique was chosen because it permits the application of high, well defined and reproducible amounts of dispersion energy, in this work 8000 J operating under the settings described in experimental section. The commercial names of the different SAS samples under study are included in Table 1. According to the information provided by the producers, the samples could contain particles sized in the μm range (Table 1). To prevent the AF4 instrument from clogging or forming bottlenecks in the system, it advisable to avoid the injection of μm-sized particles into the system. In addition to this, the maximum size of particles detectable by the MALS instrumentation used in this work was approximately 300 nm. Consequently, a filtration step with 0.45 μm size cutoff was included in the methodology. To improve the repeatability of the process the use of vacuum-assisted filtration was preferred rather than manual filtration. The impact of the filtered volume on the z-average and the total mass concentration under the established filtration conditions was studied for samples E551 5 and E551 9.

3.2. Characterization by DLS

Measurements of the hydrodynamic diameter (expressed as z-average diameter) of all the materials under study were performed by DLS before and after filtration through the 0.45 μm membrane. Values of the z-average diameter and the polydispersity index (PDI) are included in Table 1 together with their respective RSDs. In the case of the freshly-prepared unfiltered suspensions, measurements were conducted immediately after preparation of the suspensions. The z-average values oscillated between 152.3 and 202.0 nm, for the fumed SASs, and from 284.9 to 644.6 nm, for the rest. The PDI of all suspensions were above 0.400 in every case and indicated highly polydispersed samples. Measurements of the same suspensions after 24 h were also performed and the results are included in Table 1. It can be observed that the measured z-average values of pyrogenic SAS, as well as the respective PDI, showed insignificant variation after 24 h, which suggests that the suspension protocol generated reasonable stable dispersions for 24 h. For all the other samples, the z-average values decreased from 28 to 61% approximately. In the same manner, PDIs obtained after 24 h were lower than 0.244 in every case, which corresponded to a less polydispersed dispersion. These phenomena can be explained by the presence and sedimentation of big particles (aggregates or agglomerates). Additionally, the corresponding RSDs provide information about the stability of the suspensions during the measurement. The higher RSDs values obtained for just-prepared unfiltered suspensions suggest the presence of particles of relative great size which can be occasionally detected by the DLS instrument, making the intensity-based PSD change with time. The last can be observed in Figs. S2–S12 included in Supporting information, which show the intensity-based PSD together with the undersize frequency curve for all prepared suspensions.

As the presence of big particles hampers the detection of smaller particles below 100 nm, even if these are present in a greater number, samples were filtered, resuspended by immersion in an ultrasound bath and subjected again to DLS analysis. In preliminary experiments, it was observed that the ultrasound bath after the probe had a negligible impact on the DLS z-average. As was expected, measured z-average values for the filtered suspensions were considerably smaller than those for the unfiltered ones. The measured PDIs of the filtered suspensions also support the presence of less polydispersed materials with all particles below the established 0.45 μm cut-off. The lower RSDs are consistent with more

Table 1
List of SAS samples under study and particle size declared in the provided specifications (if applied); DLS z-average and polydispersity index values (PDI) of unfiltered and filtered samples. RSD correspond to 3 replicates. n.a.: not applicable.

			Unfiltered				Unfiltered 24 h				Filtered			
Code	Name/production process	Size declared (μm)	Z-avg (nm)	RSD (%)	PDI	RSD (%)	Z-avg (nm)	RSD (%)	PDI	RSD (%)	Z-avg (nm)	RSD (%)	PDI	RSD (%)
E551 1	Syloid Al-1 FP/Wet	7.2	558.4	2.5	0.615	11.7	219.5	1.6	0.090	11.6	226.7	1.6	0.147	13.7
E551 2	Syloid 244 FP/Wet	3.1	348.2	2.2	0.426	3.7	219.1	1.7	0.136	12.1	188.8	1.8	0.168	14.9
E551 3	Syloid 72 FP/Wet	5.1	527.3	4.1	0.659	24.4	206.9	0.1	0.120	16.7	178.2	0.9	0.185	12.3
E551 4	Tixosil 38/Wet	10-20	284.9	2.2	0.412	5.0	203.2	0.7	0.191	5.9	174.3	0.4	0.141	13.2
E551 5	Tixosil 43/Wet	8-10	341.0	3.4	0.479	4.1	206.2	1.5	0.180	7.3	144.4	0.5	0.250	1.6
E551 6	Tixosil 73/Wet	8-10	644.6	9.2	0.500	6.7	295.8	1.0	0.244	3.9	263.9	0.7	0.212	3.3
E551 7	Aerosil 380/Pyrogenic	n.a.	161.6	2.5	0.463	4.9	162.8	2.3	0.349	15.5	130.2	0.9	0.134	9.4
E551 8	Cab-*O*-Sil M-5F/Pyrogenic	n.a.	152.3	3.2	0.493	1.6	153.5	0.4	0.440	0.6	143.3	0.2	0.121	1.9
E551 9	Cab-*O*-Sil EH-5F/Pyrogenic	n.a.	202.0	1.4	0.454	16.4	192.2	4.6	0.445	18.2	130.0	0.1	0.132	5.9
E551 10	Tixosil 38 AB/Wet	10-20	331.8	1.7	0.447	4.8	189.7	1.1	0.157	10.0	149.0	0.2	0.229	7.5
E551 11	Tixosil 38 A/Wet	60	463.6	5.7	0.731	8.2	183.1	1.2	0.183	1.5	121.4	0.8	0.268	1.7

stable dispersions and the generated PSDs of the filtered dispersions (included in Figs. S2–S12) showed good repeatability. As Table S1 shows, when increasing the filtered volume, for non-pyrogenic SAS the z-average value decreased suggesting that the permeation of smaller particles was less affected by clogging of filters, compared to the permeation of greater ones. Such a trend was not observed for pyrogenic SAS, indicating lower polydispersity than non-pyrogenic SAS. Although the particle concentrations found in the suspensions were significantly reduced after the filtration process (which is discussed in following Section 3.3) the automatic selection of the attenuator permitted good quality measurements.

Despite of the fact that found z-averages were above 100 nm in all cases, materials under study exhibited polydispersed PSDs with particles that could potentially be in the size range below 100 nm. Although the inspection of the generated PSDs and frequency curves might serve as indicators for the assessment on the presence of nanoparticles below 100 nm, they are strongly influenced by the repeatability of the measurements and, in particular, the stability of the suspension. This fact, together with the intrinsic lack of sensitivity of DLS for small particles, limits the suitability of DLS as a preliminary positive screening technique.

3.3. Characterisation of SAS filtrates by ICPMS

The exact amount of SAS that passed through the filtration membrane was measured by ICPMS. Results of the filtration of volumes of 2 mL are summarised in Table 2 together with the recovery, which was calculated according to the following equation: (mass concentration in the filtrate/mass concentration original) × 100. Concentrations above the mg L^{-1} level were found in all cases. Differences in the recovery rates for pyrogenic and non-pyrogenic SAS were noteworthy and oscillated between highest 11.6 to lowest 0.1%, respectively. Despite of the fact that DLS allowed the detection of particles below the established cut-off, most of the solid mass content present in the original suspensions was lost during filtration. This fact can be illustratively explained according to the relative mass units per particle for spheres with diameters of (e.g.) 100, 500 and 1000 nm, which can be estimated as 1, 130 and 1000, respectively. In other words, the mass of a single particle of 1000 nm diameter is equivalent to the mass of 8 particles of 500 nm or 1000 particles of 100 nm. As Table S1 illustrates, it is important to mention that the recovery rate depends greatly on the volume of filtered suspension because as the filter becomes clogged, the particles with greater mass contribution are retained. Moreover, the filtration process ensures that no particle greater than the cut-off pore size passes through the filter but does not guarantee that the recovery of the particles smaller than the cut-off is quantitative. In this regard, the introduction of a filtration step during the characterisation of materials and subsequent assessment on potential nanomaterials should be carefully evaluated, as it impacts directly on the shape of the PSDs. The last is especially crucial if number-based quantitative information is required, as it is currently the case for the EC recommended definition of nanomaterial (EC Definition 2011/696). Pyrogenic samples yielded higher recoveries after filtration, however at the same time also showed poorer repeatability among the replicates, probably due to filter clogging during filtration. On the other hand, the filtration of non-pyrogenic SAS showed reasonable good repeatability.

3.4. Characterisation by AF4-MALS-ICPMS

As mentioned before, AF4 allows the separation of particles according to their hydrodynamic diameter within a defined dynamic size range. Moreover, the AF4 coupled on-line with a MALS detector enables the acquisition of additional, independent, information of the particle size. Thus, an AF4-MALS-ICPMS method was developed using a mild cross-flow (0.15 mL min^{-1}) in order to allow the fractionation of particles below 450 nm, which was the established cutoff. The elution profiles using MALS detection of each filtered suspension were obtained and they are included in Figs. S2–S12. The values of root mean square (rms) radii were calculated using ASTRA software for MALS and plotted in the corresponding graphs. Results are summarised in Table S2 together with the calculated values of AF4 diameter at peak maximum. Although size values obtained with different techniques are not directly comparable, in general the z-average, AF4 diameters and rms radii measured were in good agreement. With regard to this, the AF4 diameter at peak maximum can be considered as a modal value of hydrodynamic diameter, whereas z-average and rms radii are mean values of PSD. The elution profiles of most of the samples under study suggested the presence of particles with a diameter below 100 nm (see individual AF4-MALS characterisation in Figs. S2–S12). However, due to the inherent lack of sensitivity of MALS detection for the NPs in the lower size range, AF4-ICPMS was used for the detection of particles in the lower size range. Fig. 1A shows the fractograms obtained by ICPMS corresponding to the eleven materials under study. The presence of particles eluting before the 100 nm SiO_2-NPs standard can be observed. The phenomenon is more evident in Fig. 1B and C, for the detailed elution profiles of pyrogenic and non-pyrogenic materials, respectively.

In order to further investigate the size range of interest below 100 nm, a second AF4-MALS-ICPMS method was used with a higher cross-flow (1.0 mL min^{-1}), allowing the fractionation and size determination of particles with a diameter below 100 nm. The fractograms of all prepared suspensions acquired using MALS detector, as well as rms radii are included in Figs. S2–S12 and Table S2, respectively. In general, only rms radii calculated for pyrogenic SAS analysed using the method targeting particles below 100 nm

Table 2
Concentration of unfiltered and filtered samples by off-line ICPMS ($N = 3$) and AF4-ICPMS; hydrodynamic diameters obtained by AF4 calibration.

	ICPMS				AF4-ICPMS			
	Unfiltered	Filtered			Below 450 nm	Below 100 nm		
Code	C measured ($mg\,L^{-1}$)	C measured ($mg\,L^{-1}$)	Recovery (%)	RSD (%)	AF4 diameter[a] (nm)	AF4 diameter[b] (nm)	C measured[c] ($mg\,L^{-1}$)	N[d] (particle mL^{-1}) 10^{-11}
E551 1	12100	12.8	0.1	6.0	343.5	n.d.	n.d.	n.d.
E551 2	12479	29.9	0.2	14.3	291.8	20.6	3.2	3.5
E551 3	12161	68.3	0.6	7.0	296.7	28.2	18.3	7.8
E551 4	12440	32.4	0.3	7.8	277.6	22.6	6.4	5.3
E551 5	12175	81.6	0.7	2.3	243.1	39.8	34.6	5.2
E551 6	12818	29.9	0.2	1.7	294.1	23.5	0.9	0.1
E551 7	11681	1350.2	11.6	46.5	166.5	n.a.	n.a.	n.a.
E551 8	12175	468.2	3.8	42.3	188.3	n.a.	n.a.	n.a.
E551 9	12109	1211.2	10.0	35.3	197.1	n.a.	n.a.	n.a.
E551 10	12048	76.6	0.6	2.9	278.9	34.8	22.5	5.0
E551 11	12110	85.6	0.7	5.0	241.2	35.7	54.5	11.4

[a] AF4 diameter obtained by the method targeting particles below 450 nm.
[b] AF4 diameter obtained by the method targeting particles below 100 nm.
[c] Concentration of silica NPs calculated by AF4-ICPMS and prechannel calibration with NPs-standards.
[d] Number of particles estimated using the mass concentration of filtered samples (measured by AF4-ICPMS and prechannel calibration with NPs-standards) and AF4 diameter obtained by the method targeting particles below 100 nm.

diameter were in agreement with rms radii calculated using the method targeting particles below 450 nm, showing an expected reduced value due to the minor contribution of greater particles. For the rest of suspensions, the concentration of suspended material with a particle size below 100 nm was insufficiently high to be reliably measured using MALS.

ICPMS detection overcame the problem of sensitivity for small particles. In this regard, an AF4-ICPMS method previously developed and evaluated provided enough sensitivity to reliably detect SiO_2-NPs present in all the samples, within the size range between 20 and 100 nm, as it is displayed in Fig. 2A. Whereas pyrogenic SAS materials showed relatively broad eluting bands covering a size range beyond the dynamic calibration size range (Fig. 2B), the rest of the samples showed well resolved peaks which allowed the calculation of AF4 diameters at the peak maximum (Fig. 2C). Thus, it was possible to quantify the mass of nanoparticles eluting below the 100 nm size threshold using prechannel calibration with SiO_2-NPs [31]. Only in the case of the material coded as E551 1, no particulate material was detected above the limits of detection reported in Experimental section. The measured mass concentration of particles below 100 nm and the calculated AF4 diameters are summarised in Table 2. Both parameters were used to make

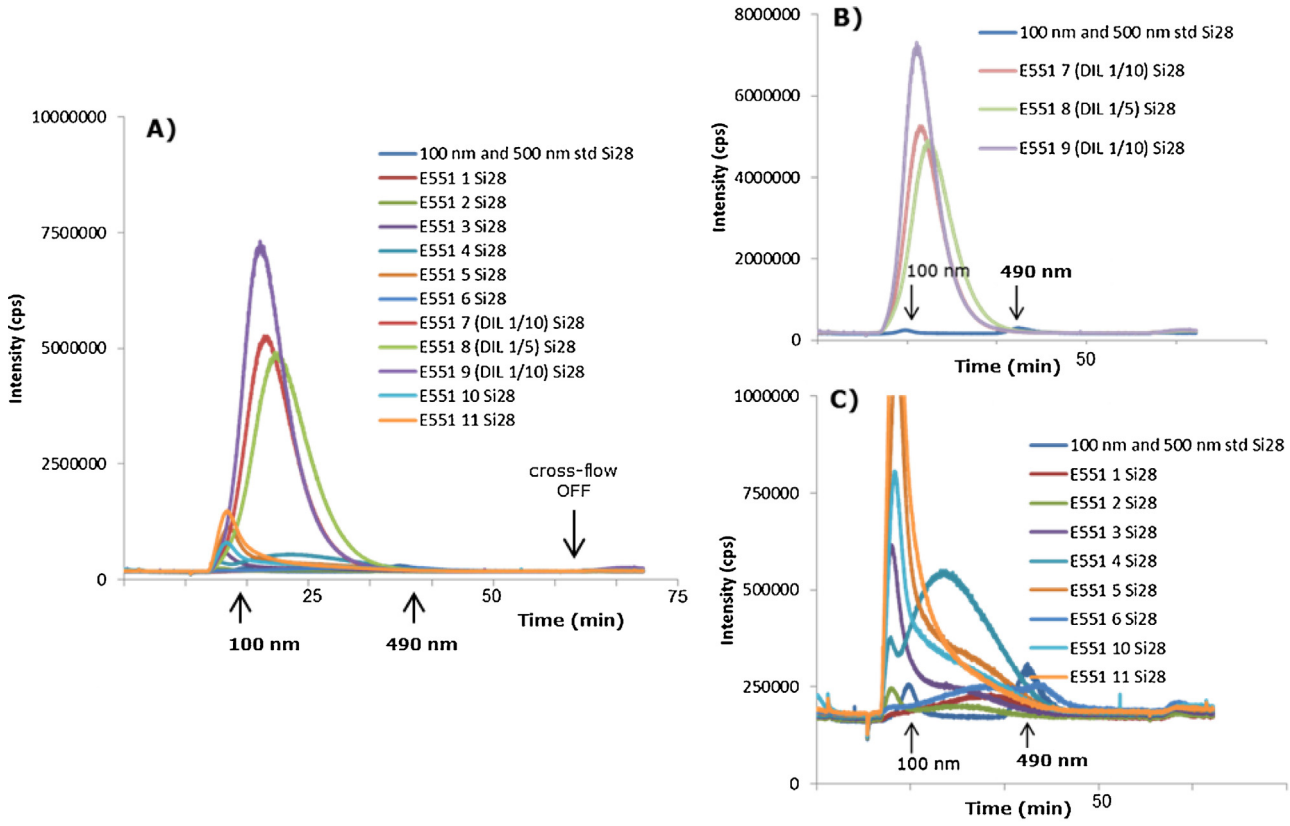

Fig. 1. Fractograms obtained after the injection of: (A) all filtered samples by AF4-ICPMS applying the method targeting particles below 450 nm; (B) detail of fractograms corresponding to pyrogenic SAS with SiO_2-NPs standards; (C) detail of fractograms corresponding to wet SAS with SiO_2-NPs standards.

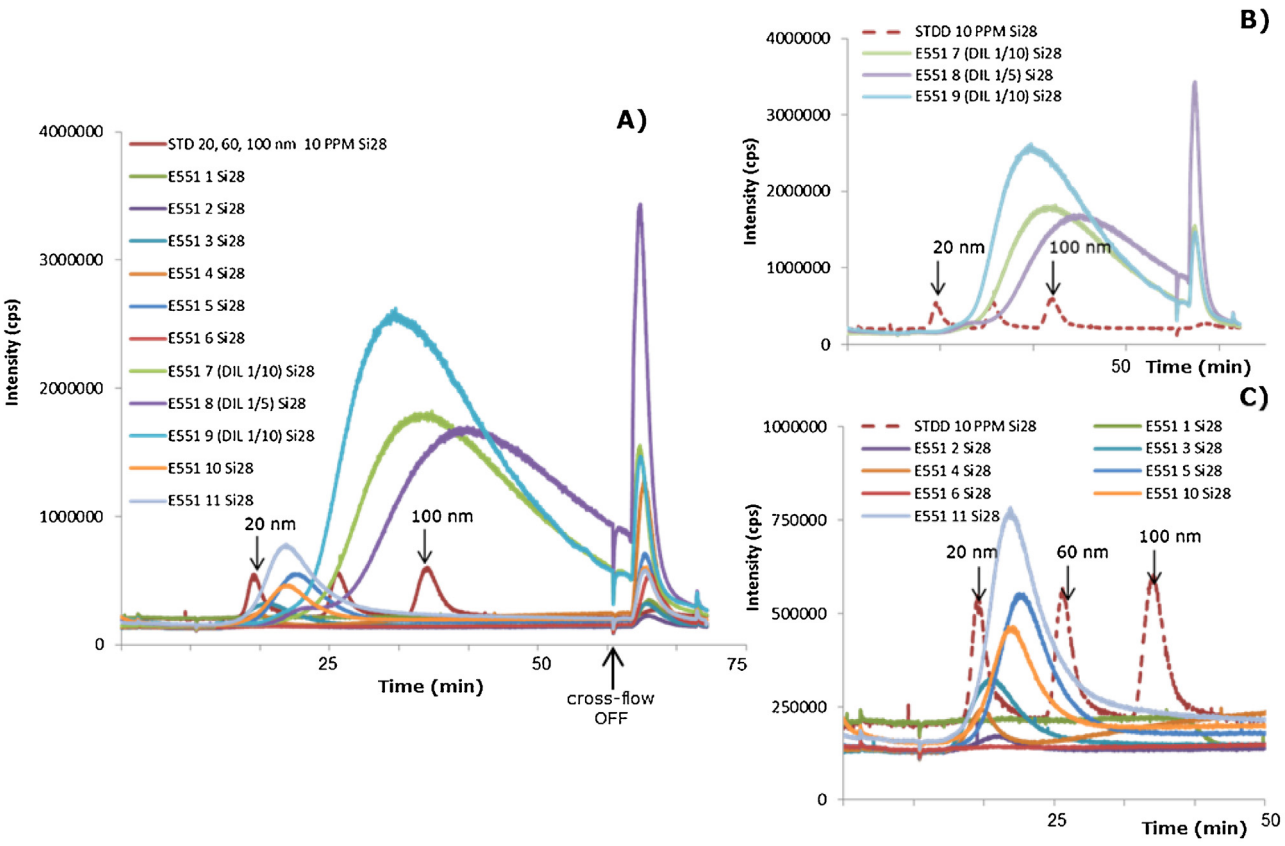

Fig. 2. Fractograms obtained after the injection of: (A) all filtered samples by AF4-ICPMS applying the method targeting particles below 100 nm; (B) detail of fractograms corresponding to pyrogenic SAS with SiO_2-NPs standards; (C) detail of fractograms corresponding to wet SAS with SiO_2-NPs standards.

an estimated conversion into number concentration by applying the corresponding AF4 diameters as PSD nominal size, assuming spherical particles and a density of 2 g mL^{-1}. The presence of NPs with equivalent hydrodynamic diameters between 20 and 40 nm can be attributed to the detection of constituent particles or small aggregates. The narrow signal visible on all fractograms of Fig. 2A is due to the material exiting the channel once the field has been removed,

3.5. Characterization by TEM

Although, in principle, TEM allows the determination of PSDs of materials regardless of the their degree of dispersity, in the case of highly polydispersed samples such a task requires an expert operator, adequate design of representative image acquisition and an exhaustive statistical analysis of data [35,36]. It should be noted that for polydispersed materials the acquisition of reliable PSDs by TEM also requires a thorough and representative sampling, meaning also the acquisition of a significant number of images with different magnification covering all the size range of particles [37], which is in some cases simply not feasible due to the intrinsic size limitations of the technique. For example, the upper size threshold for an average transmission electron microscope would be around a few tens microns while the lower size limit would be strongly affected by the chemical composition of the material. The correct determination of particle boundaries becomes more difficult when facing high noise images, which is often the case for TEM. Therefore, the higher the electron density of the material analyzed the greater the contrast difference with the background of the grid and the easier its identification. Moreover, preliminary information about the expected particle size is always desired in order to determine the most suitable sample preparation method and ensure that the images collected are representative of the sample.

In the present work, all dispersions, filtered and unfiltered, were subjected to evaluation by TEM in order to assess on the presence of SiO_2-NPs with an equivalent circle diameter (ECD i.e., the diameter of a circle with an equivalent area) of 100 nm or less. The NPs' size detection limit (smallest particle size that can be reliably distinguished from background) was estimated for each set of samples. As an illustrative example, Fig. 3 includes selected TEM images of sample E551-2 together with the TEM image analysis applying different minimum ECD thresholds and their corresponding PSDs. Fig. 3A–C represent the same material at different magnifications, which led to different size detection limits under the same analysis conditions. The PSDs resulting from size distribution analysis show that individual images are not representative of the whole sample and that they only provide information on a defined size range. In addition, a change in the minimum ECD threshold could led to false counting depending on whether background is incorrectly detected as NP, such as for example after setting minimum limits of 3 or 4 nm in Fig. 3A. Representative images for each type of material are included in Supporting information (Figs. S13–S23). According to the definition of nanomaterial in the Regulation 1169/2011 on the provision of food information to consumers no number fraction is specified, nor it is necessary to provide data which is representative of the whole size range. In this context, results of the TEM analysis are summarized in Table 3, showing that image analysis at the highest magnification allowed the detection and measurement of primary particles and small aggregates with ECD below 100 nm and above the size detection limits in all the samples under study.

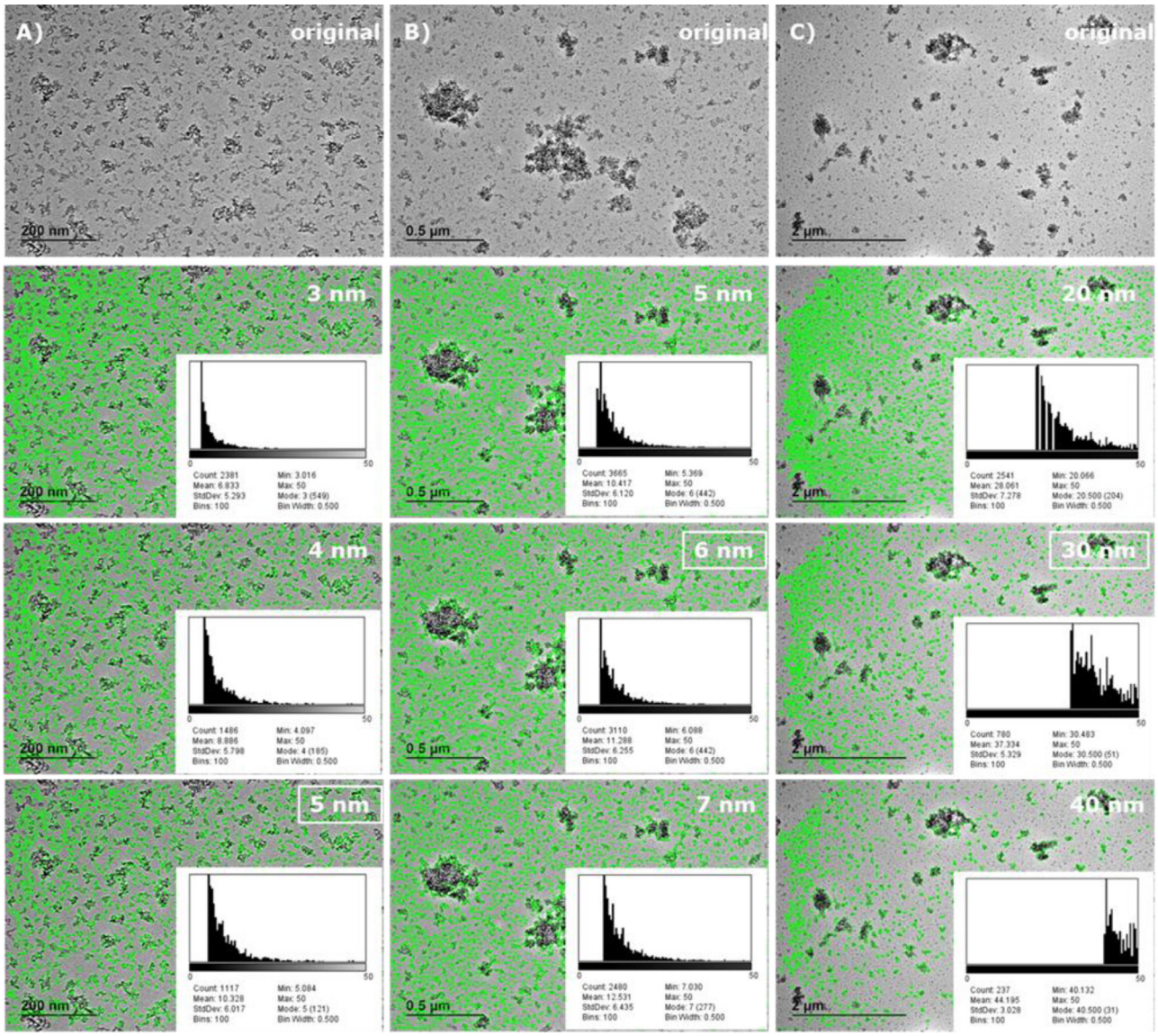

Fig. 3. TEM image analysis of sample E551 2 at different magnifications (10×, 30× and 60× for A, B and C, respectively) and different minimum ECD thresholds. Insets represent the resulting size distributions analyzed under the specified conditions in each case.

Table 3
TEM analysis including: number of counts, minimum detectable size, mode, mean of equivalent circle diameter, and relative standard deviation (%), for all samples under study.

E551	N counts	Minimum size (nm)	Mode (nm)	Mean ECD (nm)	RSD (%)
1	225	8	9	15.3	58.8
2	1117	5	5	10.3	58.3
3	364	6	7.5	15.2	55.9
4	224	9	11	21.3	49.8
5	301	7	7	16.4	59.6
6	568	7	7	17.4	56.3
7	519	6	6	15.5	59.7
8	386	6	6	13.8	61.6
9	533	6	7.5	12.3	63.4
10	292	6	6	17.2	62.2
11	179	6	6	14.1	66.7

4. Conclusions

All experiments in this work refer to food-grade SAS dispersed in water according to an established dispersing protocol. In this regard, key parameters such as type of dispersion technique, type of dispersant solution, conditions (time, temperature, energy supplied), type and chemistry of filters when used, etc. were not addressed.

DLS was well suited to provide preliminary information about the PSD of the samples. However, the quality of the measurements is strongly influenced by the velocity of sedimentation of bigger aggregates and agglomerates. Because of the poor sensitivity of DLS to small NPs, the presence of big particles tends to mask the presence of the smaller ones and therefore the technique should be only used as preliminary screening technique.

AF4 allowed the fractionation of particles according to their hydrodynamic size. MALS detection coupled to the AF4 instrument allowed the acquisition of additional independent information of the particle size (rms radii). However, the dynamic size range of application was limited and insufficient for a highly polydispersed material as SAS under study. AF4-ICPMS coupling showed that detection sensitivity was independent of particle size while the applicable size range was determined by the AF4 separation parameters. By using prechannel calibration with monodispersed SiO_2-NPs standards of known size and concentration, accurate

information about the hydrodynamic size and concentration of discrete fractions that eluted in a well-defined peak were obtained. Hence, it was possible to reliably detect SAS-NPs for ten of eleven samples. Moreover, in seven different samples, it was possible to quantify the mass concentration of eluting nanosized particles. As samples contained large aggregates, a filtration step was included prior AF4 analysis to avoid the introduction of big particles in the instrument. This operation should be always carefully evaluated if quantitative purposes (threshold number) are required. TEM showed a great size range of application, allowing the analysis of unfiltered SAS samples. It was possible to calculate experimental size limits of detection for each sample and to subsequently assess the presence of NPs below 100 nm. As was expected, TEM characterization confirmed that all the samples contained primary particles and small aggregates below 100 nm.

Nowadays, following a strict interpretation of the definition of nanomaterial in the Regulation 1169/2011 on the provision of food information to consumers, the detection of even a single NP below 100 nm would automatically require the product to be label as [nano]. All the techniques studied in this work can be used only as positive tests as their dynamic size ranges are limited by having minimum detectable size which was greater than 1 nm.

Conflict of interest

The authors declare no competing financial interest.

Appendix A. Supplementary data

Supplementary data associated with this article can be found, in the online version, at http://dx.doi.org/10.1016/j.chroma.2015.12.058.

References

[1] R. Peters, P. Brandhoff, S. Weigel, H. Marvin, H. Bouwmeester, K. Aschberger, H. Rauscher, V. Amenta, M. Arena, F. Botelho Moniz, S. Gottardo, A. Mech, Inventory of Nanotechnology Applications in the Agricultural, Feed and Food Sector, Inventory of Nanotechnology Applications in the Agricultural, Feed and Food Sector (2012).

[2] B. Nowack, T.D. Bucheli, Occurrence, behavior and effects of nanoparticles in the environment, Environ. Pollut. 150 (2007) 5–22.

[3] A. Al-Kattan, A. Wichser, R. Vonbank, S. Brunner, A. Ulrich, S. Zuin, Y. Arroyo, L. Golanski, B. Nowack, Characterization of materials released into water from paint containing nano-SiO_2, Chemosphere 119 (2015) 1314–1321.

[4] B. Nowack, C. Brouwer, R.E. Geertsma, E.H.W. Heugens, B.L. Ross, M.C. Toufektsian, S.W.P. Wijnhoven, R.J. Aitken, Analysis of the occupational, consumer and environmental exposure to engineered nanomaterials used in 10 technology sectors, Nanotoxicology 7 (2013) 1152–1156.

[5] Regulation (EC) No 1333/2008 on food additives, Official Journal of the European Union, L 354/16. (2008).

[6] Regulation (EU) No 1169/2011 on the provision of food information to consumers, Official Journal of the European Union, L 3014/18. (2011).

[7] Commission Recommendation of 18 October 2011 on the definition of nanomaterial (2011/696/EU), Official Journal of the European Union, L275/38. (2011).

[8] S. Dekkers, H. Bouwmeester, P.M.J. Bos, R.J.B. Peters, A.G. Rietveld, A.G. Oomen, Knowledge gaps in risk assessment of nanosilica in food: evaluation of the dissolution and toxicity of different forms of silica, Nanotoxicology 7 (2013) 367–377.

[9] J.H. Lim, P. Sisco, T.K. Mudalige, G. Sánchez-Pomales, P.C. Howard, S.W. Linder, Detection and characterization of SiO_2 and TiO_2 nanostructures in dietary supplements, J. Agric. Food Chem. 63 (2015) 3144–3152.

[10] S. Dekkers, P. Krystek, R.J.B. Peters, D.P.K. Lankveld, B.G.H. Bokkers, P.H. Van Hoeven-Arentzen, H. Bouwmeester, A.G. Oomen, Presence and risks of nanosilica in food products, Nanotoxicology 5 (2011) 393–405.

[11] R. Peters, E. Kramer, A.G. Oomen, Z.E. Herrera Rivera, G. Oegema, P.C. Tromp, R. Fokkink, A. Rietveld, H.J.P. Marvin, S. Weigel, A.A.C.M. Peijnenburg, H. Bouwmeester, Presence of nano-sized silica during in vitro digestion of foods containing silica as a food additive, ACS Nano 6 (2012) 2441–2451.

[12] S.C. Yang, S.Y.R. Paik, J. Ryu, K.O. Choi, T.S. Kang, J.K. Lee, C.W. Song, S. Ko, Dynamic light scattering-based method to determine primary particle size of iron oxide nanoparticles in simulated gastrointestinal fluid, Food Chem. 161 (2014) 185–191.

[13] A. Braun, O. Couteau, K. Franks, V. Kestens, G. Roebben, A. Lamberty, T.P.J. Linsinger, Validation of dynamic light scattering and centrifugal liquid sedimentation methods for nanoparticle characterisation, Adv. Powder Technol. 22 (2011) 766–770.

[14] C. Nickel, J. Angelstorf, R. Bienert, C. Burkart, S. Gabsch, S. Giebner, A. Haase, B. Hellack, H. Hollert, K. Hund-Rinke, D. Jungmann, H. Kaminski, A. Luch, H.M. Maes, A. Nogowski, M. Oetken, A. Schaeffer, A. Schiwy, K. Schlich, M. Stintz, F. Von Der Kammer, T.A.J. Kuhlbusch, Dynamic light-scattering measurement comparability of nanomaterial suspensions, J. Nanopart. Res. 16 (2014) 1–12.

[15] F. Katrin, B. Adelina, C.-G. Jean, C. Olivier, K. Vikram, L.M. Andree, L. Thomas, R. Gert, Certification of the equivalent spherical diameters of silica nanoparticles in aqueous solution—Certified Reference Material ERM®-FD304, EC, Joint Research Centre, Institute for Reference Materials and Measurements (2012).

[16] S. Tadjiki, S. Assemi, C.E. Deering, J.M. Veranth, J.D. Miller, Detection, separation, and quantification of unlabeled silica nanoparticles in biological media using sedimentation field-flow fractionation, J. Nanopart. Res. 11 (2009) 981–988.

[17] K. Tiede, A.B.A. Boxall, D. Tiede, S.P. Tear, H. David, J. Lewis, A robust size-characterisation methodology for studying nanoparticle behaviour in 'real' environmental samples, using hydrodynamic chromatography coupled to ICP-MS, J. Anal. At. Spectrom. 24 (2009) 964–972.

[18] J. Gigault, J.M. Pettibone, C. Schmitt, V.A. Hackley, Rational strategy for characterization of nanoscale particles by asymmetric-flow field flow fractionation: a tutorial, Anal. Chim. Acta 809 (2014) 9–24.

[19] S. Dubascoux, F. Von Der Kammer, I. Le Hécho, M.P. Gautier, G. Lespes, Optimisation of asymmetrical flow field flow fractionation for environmental nanoparticles separation, J. Chromatogr. A 1206 (2008) 160–165.

[20] M.S. Jiménez, M.T. Gómez, E. Bolea, F. Laborda, J. Castillo, An approach to the natural and engineered nanoparticles analysis in the environment by inductively coupled plasma mass spectrometry, Int. J. Mass Spectrom. 307 (2011) 99–104.

[21] E.P. Gray, T.A. Bruton, C.P. Higgins, R.U. Halden, P. Westerhoff, J.F. Ranville, Analysis of gold nanoparticle mixtures: a comparison of hydrodynamic chromatography (HDC) and asymmetrical flow field-flow fractionation (AF4) coupled to ICP-MSysis of gold nanoparticle mixtures: a comparison of hydrodynamic chromatography (HDC) and asymmetrical flow field-flow fractionation (AF4) coupled to ICP-MS, J. Anal. At. Spectrom. 27 (2012) 1532–1539.

[22] C. Contado, L. Ravani, M. Passarella, Size characterization by sedimentation field flow fractionation of silica particles used as food additives, Anal. Chim. Acta 788 (2013) 183–192.

[23] F.V.D. Kammer, S. Legros, T. Hofmann, E.H. Larsen, K. Loeschner, Separation and characterization of nanoparticles in complex food and environmental samples by field-flow fractionation, TrAC—Trends Anal. Chem. 30 (2011) 425–436.

[24] J.C. Giddings, Field-flow fractionation: analysis of macromolecular, colloidal, and particulate materials, Science 260 (1993) 1456–1465.

[25] S. Wagner, S. Legros, K. Loeschner, J. Liu, J. Navratilova, R. Grombe, T.P.J. Linsinger, E.H. Larsen, F. Von Der Kammer, T. Hofmann, First steps towards a generic sample preparation scheme for inorganic engineered nanoparticles in a complex matrix for detection, characterization, and quantification by asymmetric flow-field flow fractionation coupled to multi-angle light scattering and ICP-MS, J. Anal. At. Spectrom. 30 (2015) 1286–1296.

[26] B. Meermann, Field-flow fractionation coupled to ICP-MS: separation at the nanoscale, previous and recent application trends, Anal. Bioanal. Chem. 407 (2015) 2665–2674.

[27] H. Bouwmeester, P. Brandhoff, H.J.P. Marvin, S. Weigel, R.J.B. Peters, State of the safety assessment and current use of nanomaterials in food and food production, Trends Food Sci. Technol. 40 (2014) 200–210.

[28] H. Hagendorfer, R. Kaegi, M. Parlinska, B. Sinnet, C. Ludwig, A. Ulrich, Characterization of silver nanoparticle products using asymmetric flow field flow fractionation with a multidetector approach—a comparison to transmission electron microscopy and batch dynamic light scattering, Anal. Chem. 84 (2012) 2678–2685.

[29] C. Cascio, D. Gilliland, F. Rossi, L. Calzolai, C. Contado, Critical experimental evaluation of key methods to detect, size and quantify nanoparticulate silver, Anal. Chem. 86 (2014) 12143–12151.

[30] D. Bartczak, P. Vincent, H. Goenaga-Infante, Determination of size- and number-based concentration of silica nanoparticles in a complex biological matrix by online techniques, Anal. Chem. 87 (2015) 5482–5485.

[31] F. Barahona, O. Geiss, P. Urbán, I. Ojea-Jimenez, D. Gilliland, J. Barrero-Moreno, Simultaneous determination of size and quantification of silica nanoparticles by asymmetric flow field-flow fractionation coupled to ICPMS using silica nanoparticles standards, Anal. Chem. 87 (2015) 3039–3047.

[32] P. Bihari, M. Vippola, S. Schultes, M. Praetner, A.G. Khandoga, C.A. Reichel, C. Coester, T. Tuomi, M. Rehberg, F. Krombach, Optimized dispersion of nanoparticles for biological in vitro and in vivo studies, Part. Fibre Toxicol. 5 (2008) 14.

[33] J.S. Taurozzi, V.A. Hackley, M.R. Wiesner, Ultrasonic dispersion of nanoparticles for environmental, health and safety assessment issues and recommendations, Nanotoxicology 5 (2011) 711–729.

[34] J.B. Vicent Pena, K. Kund, U. Hempelmann, W. Wohlleben, T. Koch, A. Burke, G. McNulty, A. Hartl-Gunselmann, S. Knobl, M. Reisinger, D. Gilliland, P. Gisbson, B. Sokull-Kluettgen, H. Stamm, H. Liewald, Basic Comparison of Particle Size Distribution Measurements of Pigments and Fillers Using Commonly

Available Industrial Methods, EC, JRC, Institute for Health and Consumer Protection, 2014.
[35] A. Dudkiewicz, A.B.A. Boxall, Q. Chaudhry, K. Mølhave, K. Tiede, P. Hofmann, T.P.J. Linsinger, Uncertainties of size measurements in electron microscopy characterization of nanomaterials in foods, Food Chem. 176 (2015) 472–479.
[36] T.P.J. Linsinger, Q. Chaudhry, V. Dehalu, P. Delahaut, A. Dudkiewicz, R. Grombe, F. Von Der Kammer, E.H. Larsen, S. Legros, K. Loeschner, R. Peters, R. Ramsch, G. Roebben, K. Tiede, S. Weigel, Validation of methods for the detection and quantification of engineered nanoparticles in food, Food Chem. 138 (2013) 1959–1966.
[37] A. Dudkiewicz, K. Tiede, K. Loeschner, L.H.S. Jensen, E. Jensen, R. Wierzbicki, A.B.A. Boxall, K. Molhave, Characterization of nanomaterials in food by electron microscopy, TrAC—Trends Anal. Chem. 30 (2011) 28–43.